Reprinted from

EARTH AND PLANETARY SCIENCE LETTERS

Earth and Planetary Science Letters 173 (1999) 413–424

Analysis of poorly stratified lateritic terrains overlying a granitic bedrock in West Africa, using 2-D electrical resistivity tomography

Anicet Beauvais [a,*], Michel Ritz [b], Jean-Claude Parisot [b], Michel Dukhan [b], Christian Bantsimba [b,c]

[a] IRD, Département RED, UR-062, Centre d'Ile de France, 32 avenue Henri Varagnat, 93143 Bondy Cedex, France
[b] IRD, Département RED, UR-062, Centre de Hann, B.P. 1386, Dakar, Senegal
[c] IRD, Département RED, UR-062, UCAD, Département de Géologie, Dakar, Senegal

Received 11 June 1999; revised version received 1 October 1999; accepted 1 October 1999

ELSEVIER

EARTH AND PLANETARY SCIENCE LETTERS

PUBLICATION INFORMATION

Earth and Planetary Science Letters (ISSN 0012-821X). For 1999 volumes 164–173 are scheduled for publication. Subscription prices are available upon request from the publisher. Subscriptions are accepted on a prepaid basis only and are entered on a calendar year basis. Issues are sent by surface mail except to the following countries where air delivery via SAL is ensured: Argentina, Australia, Brazil, Canada, Hong Kong, India, Israel, Japan, Malaysia, Mexico, New Zealand, Pakistan, PR China, Singapore, South Africa, South Korea, Taiwan, Thailand, USA. For all other countries airmail rates are available upon request. Claims for missing issues must be made within six months of our publication (mailing) date.

Orders, claims, product enquiries: please contact the Customer Support Department at the Regional Sales Office nearest to you:

New York: Elsevier Science, PO Box 945, New York, NY 10159-0945, USA; phone: (+1) (212) 633 3730, [toll free number for North American customers: 1-8884ES-INFO (437-4636)]; fax: (+1) (212) 633 3680; e-mail: usinfo-f@elsevier.com
Amsterdam: Elsevier Science, PO Box 211, 1000 AE Amsterdam, The Netherlands; phone: (+31) 20 4853757; fax: (+31) 20 4853432; e-mail: nlinfo-f@elsevier.nl
Tokyo: Elsevier Science, 9-15 Higashi-Azabu 1-chome, Minato-ku, Tokyo 106-0044, Japan; phone: (+81) (3) 5561 5033; fax: (+81) (3) 5561 5047; e-mail: info@elsevier.co.jp
Singapore: Elsevier Science, No. 1 Temasek Avenue, #17-01 Millenia Tower, Singapore 039192; phone: (+65) 434 3727; fax: (+65) 337 2230; e-mail: asiainfo@elsevier.com.sg
Rio de Janeiro: Elsevier Science, Rua Sete de Setembro 111/16 Andar, 20050-002 Centro, Rio de Janeiro - RJ, Brazil; phone: (+55) (21) 509 5340; fax: (+55) (21) 509 1991; e-mail: elsevier@campus.com.br [Note (Latin America): for orders, claims and help desk information, please contact the Regional Sales Office in New York as listed above]

US mailing notice: *Earth and Planetary Science Letters* (ISSN 0012-821X) is published twice monthly by Elsevier Science B.V., Molenwerf 1, P.O. Box 211, 1000 AE Amsterdam, The Netherlands. The annual subscription price in the USA is US $2490 (US$ price valid in North, Central and South America). Periodicals postage paid at Jamaica, NY 11431. **USA POSTMASTERS:** Send address changes to *Earth and Planetary Science Letters*, Publications Expediting Inc., 200 Meacham Avenue, Elmont, NY 11003. **AIRFREIGHT AND MAILING** in the USA by Publications Expediting Inc., 200 Meacham Avenue, Elmont, NY 11003.

ELSEVIER

Earth and Planetary Science Letters 173 (1999) 413–424

EPSL

www.elsevier.com/locate/epsl

Analysis of poorly stratified lateritic terrains overlying a granitic bedrock in West Africa, using 2-D electrical resistivity tomography

Anicet Beauvais [a,*], Michel Ritz [b], Jean-Claude Parisot [b], Michel Dukhan [b], Christian Bantsimba [b,c]

[a] *IRD, Département RED, UR-062, Centre d'Ile de France, 32 avenue Henri Varagnat, 93143 Bondy Cedex, France*
[b] *IRD, Département RED, UR-062, Centre de Hann, B.P. 1386, Dakar, Senegal*
[c] *IRD, Département RED, UR-062, UCAD, Département de Géologie, Dakar, Senegal*

Received 11 June 1999; revised version received 1 October 1999; accepted 1 October 1999

Abstract

Two-dimensional electrical resistivity tomography has been employed to investigate the subsurface structure of a thick lateritic weathering mantle overlying a granitic bedrock in southeastern Senegal. The resistivities were measured along two kilometric profiles insuring continuous coverage. Exploration pits exposed the different weathering layers, i.e., a saprolite, a mottled zone, a soft ferricrete and a ferricrete, whose respective thicknesses were used to constrain the measured apparent resistivity, despite their spatial variations. Colour-modulated pseudo-sections of apparent resistivity versus pseudo-depth including the groundsurface topography clearly show spatial variations in electrical properties of the weathering layers since their apparent resistivity changes faster than their respective thickness. The data from a cross-borehole survey along with estimates of resistivity for aquifers and granite were integrated into the pseudo-sections to provide more useful results about the real resistivity ranges of the weathering layers. The resulting geo-electrical images document the geometric relations between the different layer boundaries, in particular those of the aquifers with the bedrock and groundsurface topographies. The spatial relationships between the granitic bedrock and groundsurface topographies suggest that a large part of the actual lateritic weathering mantle is allochthonous. This also implies that the actual topography of the bedrock surface was mainly shaped by weathering processes while the hillslope geomorphic patterns result from erosion processes or lateritic weathering of reworked materials leading to ferricrete development according to the different landforms observed. It is suggested that climatic changes were implied in the landscape evolution of our study area.

Keywords: resistivity; tomography; weathering; saprolite; laterites; geomorphology; Senegal

1. Introduction

Lateritic overburden of tropical areas has been developed on many kinds of parent rocks under the effect of weathering processes. At least one third of the Earth's surface has undergone lateritic weathering processes that have led to the formation of laterites, i.e., tropical soils, bauxites and ferricretes, since the Mesozoic [1–6]. Such residual formations commonly exhibit thicknesses of several tens of metres with a complex layer organization due to vertical

* Corresponding author. Tel.: +33-1-4802-5500; Fax: +33-1-4847-3088; E-mail: beauvais@bondy.ird.fr

0012-821X/99/$ – see front matter
PII: S0012-821X(99)00245-9

and lateral variations of the geochemical and physical properties of each weathering layer [5,7]. The factors and processes governing these variations have been studied in detail in West and Central Africa on the basis of petrographical observations in pits, and of mineralogical and geochemical data [8–14]. Although such studies are useful in understanding the mechanisms of formation and transformation of the weathering layers and facies at the scale of vertical profiles, they do not provide a full knowledge of the weathering mantle, its thickness and 2-D layer organization including the geometry of the saturated domains and of the water tables [15]. Also they do not allow the interpretation of the underlying lithologic and hydrologic processes at the scale of interfluves of kilometric size. Such a knowledge is however needed in groundwater prospecting, mineral exploration and geologic mapping in the tropical shields [16,17].

The aim of our study is to provide geo-electrical sections of the lateritic overburden along a complete interfluve in order to obtain a 2-D integrated image of the geomorphological and hydrogeological structures that can document the relationships between the layer boundaries of the lateritic weathering mantle and the bedrock and groundsurface topographies.

Direct-current (DC) resistivity methods are usually applied to detect subsurface geologic and/or hydrologic anomalies. They also provide a coarse geo-electrical image of the soil surface layers and of the weathered zone [15]. The resulting 1-D models roughly display three geo-electrical layers assuming a stratified earth [18,19], with a low-resistivity layer attributed to a saprolite layer sandwiched between two resistive layers corresponding to the underlying unweathered bedrock and to the overlying ferruginous layers, e.g., the ferricrete. *Ferricrete* is used here as a generic term for ferruginous duricrust independently of the staked processes [5,7]. The deep and old weathering mantles capped with ferricretes can however exhibit significant lithological variations [5,20].

The application of the electrical resistivity tomography (ERT) method has proved useful to investigate the complex 2-D organization of poorly stratified lateritic overburden [21,22]. Two-D models resulting from ERT applications are more appropriate to investigate the deep weathering mantles since they are able to document at once the vertical and lateral variations of resistivity, whereas 1-D models from the DC method are based on limited measurements of the apparent resistivity and thus only display the coarse geo-electrical contrasts.

2. Site description

The field work was done at Tenkoto within a gold mining prospecting area in southeastern Senegal (Fig. 1). The geological basement of this area is composed of early Palaeoproterozoic formations including a greenstone belt surrounding a granitic batholith intrusion (Fig. 1A). The study is focused on the granitic intrusion overlain by a thick lateritic weathering mantle capped with ferricrete. On the basis of petrographical observations in pits, the ferricrete layer is thought to result, in large measure, from the erosion and redisposition of an earlier lateritic weathering mantle developed on the greenstones [23]. That interpretation was, however, contradicted by later researchers who argued that the lateritic weathering profiles have been developed in situ on parent rock without any allochthonous deposits [8,9]. These two opposed interpretations imply that the hillslope shape is mainly controlled by either mechanical erosion or geochemical weathering processes depending on whether one considers the first or the second proposition. One hopes to obtain useful data from ERT to resolve this issue.

The geomorphology of the greenstones area consists of steep hills, one of them bearing a ferricrete thought to be of Pliocene age [23] (Fig. 1). The hills dominate a geomorphologic system of plateaus and glacis on the granitic batholith corresponding to the 'High-Glacis' and 'Middle-Glacis', respectively, as defined by Michel [23]. Granite domes and boulders outcrop in the thalwegs around the village of

Fig. 1. (A) Location and geomorphological characteristics of the study area. According to Michel [23], the probable limit of the granitic batholith within the greenstone area is delineated by the curved line; black star stands for Tenkoto village. (B) Topographic cross section according to the dashed line in (A).

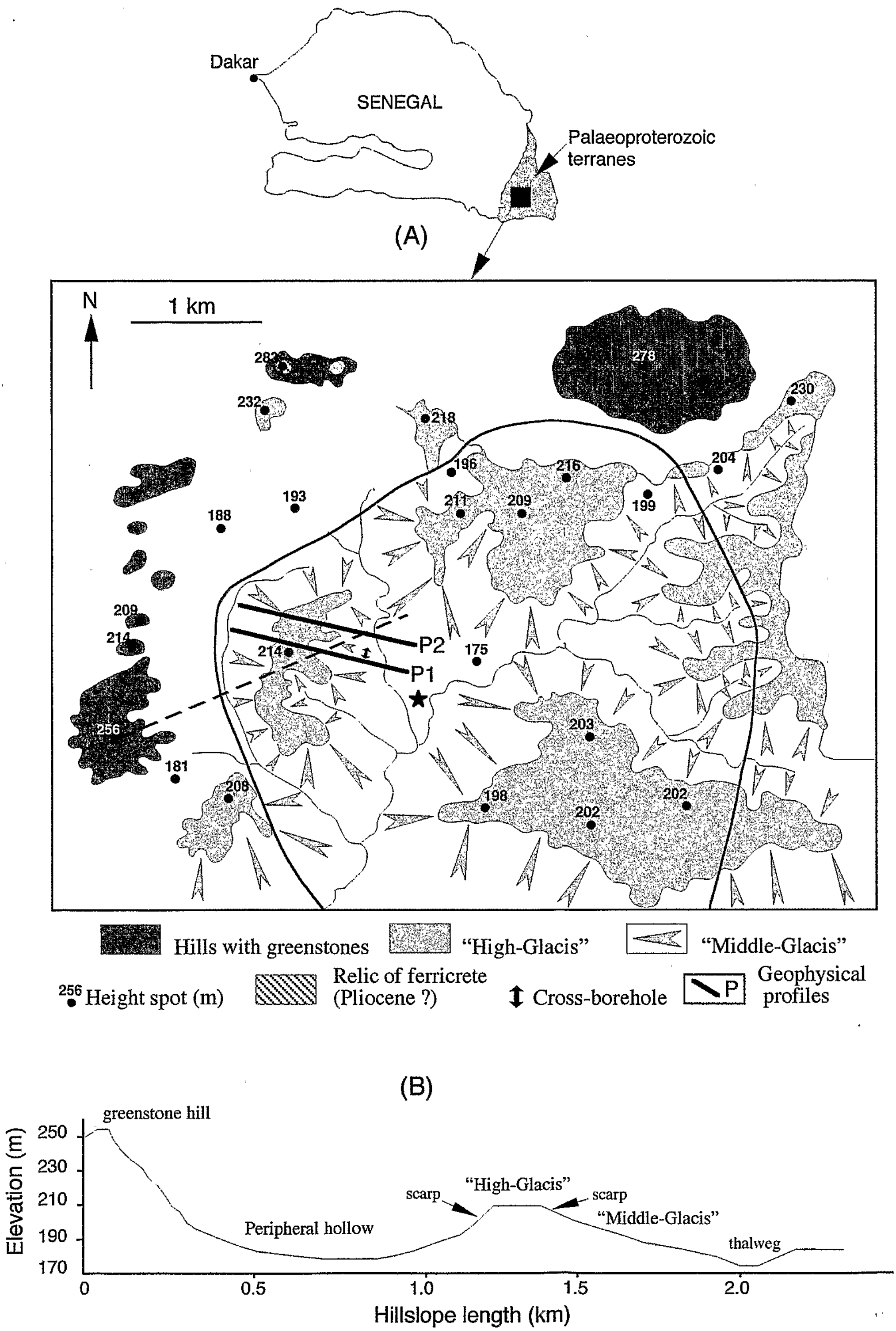
Dakar
SENEGAL
Palaeoproterozoic terranes
(A)
N
1 km
278
230
232
218
204
196
216
193
188
211
209
199
209
214
P2
214
175
P1
256
203
181
208
198
202
202
Hills with greenstones
"High-Glacis"
"Middle-Glacis"
256 Height spot (m)
Relic of ferricrete (Pliocene ?)
Cross-borehole
P
Geophysical profiles
(B)
greenstone hill
Elevation (m)
250
230
210
190
170
scarp
"High-Glacis"
scarp
"Middle-Glacis"
Peripheral hollow
thalweg
0
0.5
1.0
1.5
2.0
Hillslope length (km)

Tenkoto. The highest hills culminate around 255–285 m, while 'High-Glacis' and 'Middle-Glacis' stand at 200–215 m and 175–195 m, respectively (Fig. 1). A wide peripheral hollow in which one can find debris and blocks of greenstones and ferricrete lies down between the 'High-Glacis' and the greenstone hills (Fig. 1B). This area underwent and still undergoes active gold artisanal prospecting using pits dug along the thalwegs as well as intensive exploration by a multinational mining company. The thalwegs are flat and they were completely dry during the geo-electrical survey. Four standard layers were observed from the bottom to the top of pits: a saprolite, a mottled zone, a soft ferricrete, and a ferricrete which can present degradation facies resulting from the disaggregation of the matrix. This profile layout was used to calibrate the geo-electrical measures, in particular those obtained by the cross-borehole configuration.

The climate is seasonal tropical with a wet season from April–May to September–October and a dry season for the rest of the year. The mean annual rainfall is 1200–1300 mm, the mean annual temperature is ~28°C while the mean annual relative air humidity is ~50%. The vegetation consists of a semi-humid savanna with an alternation of wood and Graminaceae domains.

3. Geo-electric method

The ERT method was applied to provide useful information about the ranges of resistivity, ρ, for each layer composing the geo-electrical structure that best characterizes the lateritic weathering mantle. A 2-D resistivity tomography was obtained by employing the ABEM Lund Imaging System using a multi-electrode Wenner configuration with an array of 64 steel electrodes. Two profiles of 1420 m length oriented S70°E and spaced 200 m apart were investigated (Fig. 1A). They cross the 'High-Glacis' and the 'Middle-Glacis'. Profile II crosses the gently sloping north edge of the 'High-Glacis'. The unit electrode spacing was 10 m that provided a global view of hundred metres thickness of geological structures. Such a disposition is effectively appropriate to investigate the spatial relations between the layer boundaries and the groundsurface topography. Each profile was partitioned into three sections with two overlappings of 24 electrodes, i.e., 240 m. The topography of the profiles was obtained using a clinometer with measurements every 10 m and less when it was necessary. The electrical measures were made using a computer-controlled multichannel resistivity-meter located in the middle of the 64 electrodes configuration, implying that, for each section of 640 m length, the first electrode is positioned at −315 m while the last one is at 325 m [24]. The apparent resistivity data were inverted using a least-square method to obtain a pseudo-resistivity section of the underlying structures including the topographic variations [25–27]. The gradual changes of resistivity does not necessarily indicate gradual changes of the geophysical properties of the weathering layer and facies, impeding useful selection of the layer boundaries.

That has led us to carry out a cross-borehole survey between two pits spaced 10 m apart, with an electrode spacing of 0.5 m (Fig. 2). The electrodes were set up on the pit walls and in the groundsurface making an inverted U-shape electrode bridge. The cross-borehole data inversion provided the true resistivity range of the different weathering layers previously described in the pits. The resistivity of the granite was estimated using in situ measurements with small Wenner layouts while the water conductivity was directly measured in pits recently bored.

Then, the new resistivity data were incorporated into the previous inverted pseudo-resistivity sections to obtain a 2-D geo-electrical image of the lateritic weathering mantle with relatively precise limits between resistivity domains representing the different weathering layers. These geo-electrical images document on the spatial relationships between the layers, their boundaries and the topographic groundsurface, that can provide useful data to reconcile previous interpretations [8,9,23].

4. Results and discussion

4.1. Electrical resistivity tomography of the lateritic weathering mantle

The field cross-borehole results are shown in Fig. 2. The 2-D cross-borehole image obtained be-

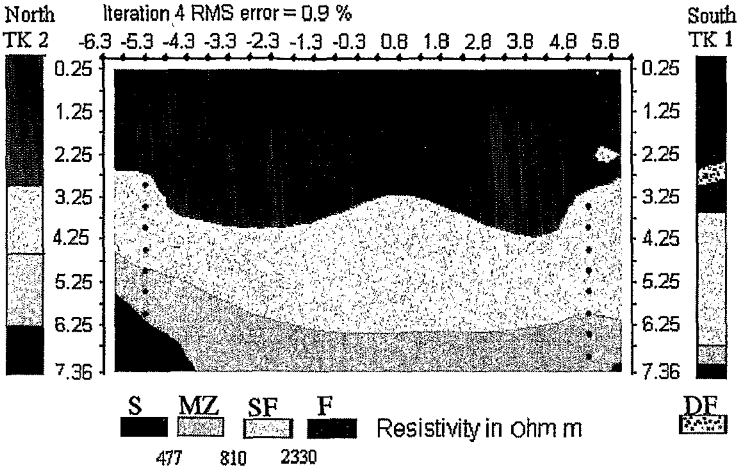

Fig. 2. Correlation between lithology of two pits (*TK 1* and *TK 2*) and the model obtained after the inversion of the cross-borehole data set. A spacing between the electrodes (dots) of 0.5 m was used. *S* = saprolite; *MZ* = mottled zone; *SF* = soft ferricrete; *F* = ferricrete; *DF* = disaggregated ferricrete. Horizontal and vertical scales in metres. Numbers below boxes are resistivities in ohm m.

tween two pits is consistent with the field observations, allowing the geo-electrical distinction of the ferricrete with $\rho > 2330$ ohm m (Ω m) from the soft ferricrete with $810 < \rho < 2330$ Ω m, and the mottled zone of $477 < \rho < 810$ Ω m from the saprolite whose $\rho < 477$ Ω m (Fig. 2). Notice that the degradation zone within the ferricrete exhibits a resistivity similar to the soft ferricrete.

2-D inversion sections of profiles I and II exhibit considerable details of the weathering layer organization (Fig. 3). This figure basically shows three layers with the first and third having relatively high resistivities, $\rho > \sim 800$ Ω m. The high resistivity is interpreted to characterize the ferruginous layers and the more or less weathered granite, respectively. The intermediate layer of lower resistivity represents the saprolite. The highest surface resistivities were measured on the topographic heights, and they seem to be thicker in the first profile than in the second one along a section ranging from ~325 to 645 m (Fig. 3). Discontinuities of saprolite resistivity are detected in profile I at 5 m, 395 m, and 705–715 m (Fig. 3A). These discontinuities are also detected in profile II at 5 m, 325 m and 355 m (Fig. 3B). They occur just above relatively sharp highs of the resistive deep layer reflecting the unweathered granite, in particular at 5 and 325 m in the second profile (Fig. 3B). Between 5 and 325 m, the deep highly resistive layers attributed to the bedrock are indeed shallower in the second profile than in the first one (Fig. 3). On the other hand, the highly resistive layers lie deeper in the second profile between ~645 and 965 m, making the low-resistivity layers look thicker (Fig. 3B). Layers of very low resistivity ranging from 7 to 40 Ω m at the two extreme ends of the profiles reflect saturated domains, i.e., between −285 and −115 m, and between 945 and 1045 in profile I (Fig. 3A), and between −25 and 285 m, 5 and 185 m, and 875 and 1065 m in profile II (Fig. 3B).

4.2. Aquifers and granite resistivities

On the basis of in situ measurements, the weathered granite is characterized by $710 < \rho < 1700$ Ω m while the unweathered granite has $\rho > 3140$ Ω m. Laboratory measurements show a mean clay content of ~30% in the pits located downslope of the 'Middle-Glacis' where the mean porosity is ~40%. The analysis of water in the pits provides a mean resistivity of 155 Ω m. These informations along with the assumption that the saprolite is roughly homogeneous were used to derive an empirical relation from the generalized Archie law [28] in order to delineate the boundaries of saturated domains in the saprolite and around the thalwegs. A more accurate estimate for the upper limit of the saturated domain resistivity is obtained by correcting for the clay contribution [25]. This relation to the ERT results indicates that a

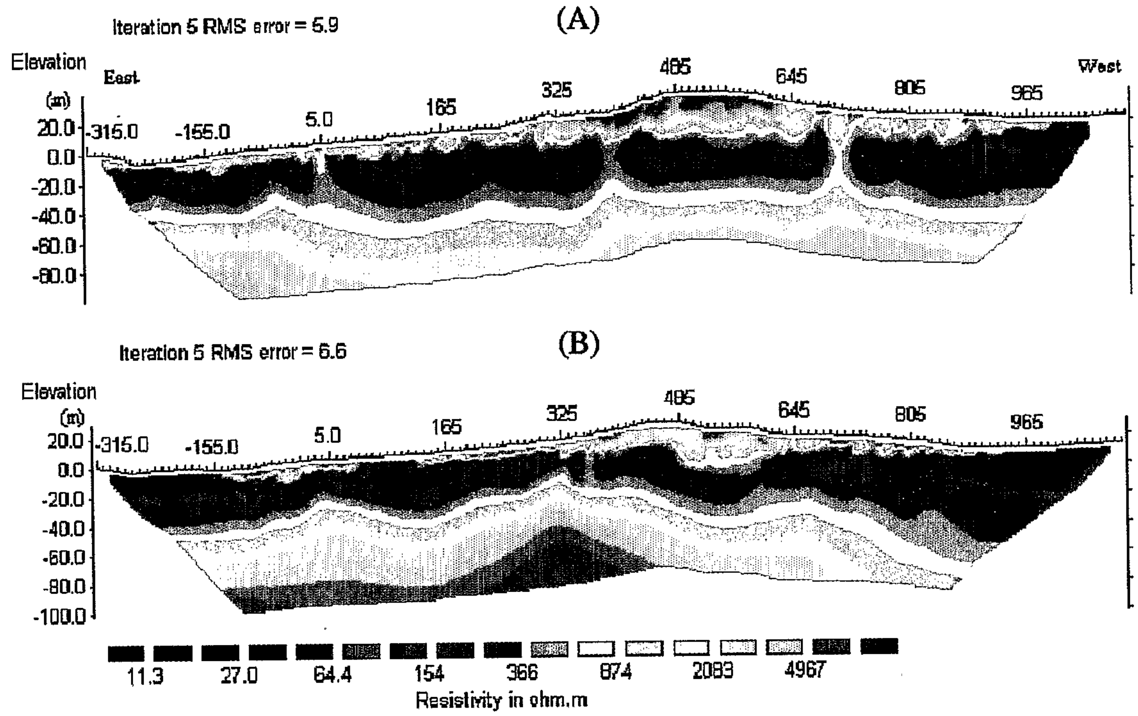

Fig. 3. 2-D inversion results including the topography with an electrode spacing of 10 m for (A) profile I and (B) profile II. Vertical exaggeration in models is 2.0.

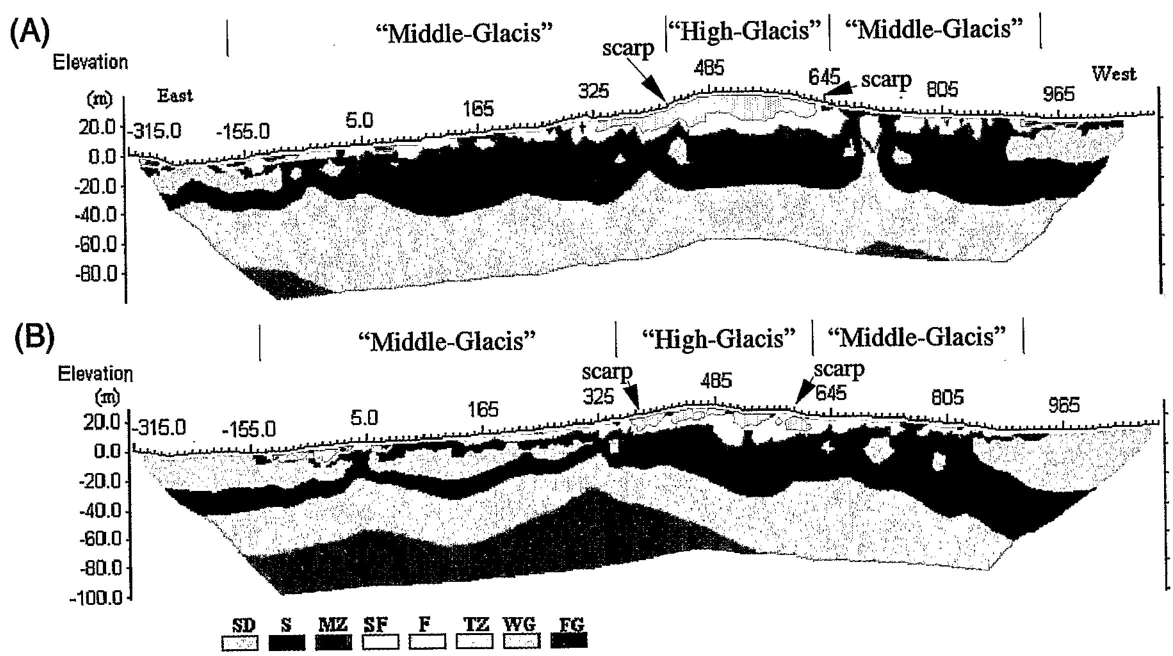

saprolite with a mean porosity of ~40%, containing ~30% clay and saturated by fluids with a mean resistivity of 155 Ω m can be reasonably described by $\rho = 130\ \Omega$ m.

4.3. Geometric relations between the layer boundaries and the groundsurface

Integrated cross sections were obtained from the interpreted ERT and cross-borehole data incorporating the aquifers and granite resistivities. These sections result in identifying eight resistivity layers as, a saturated domain, a saprolite, a mottled zone, a soft ferricrete, a ferricrete, a transition zone, a more or less weathered granite, and an unweathered granite (Fig. 4).

The first profile roughly exhibits a smooth bedrock topography while the second shows a more convex bedrock surface. Between −315 and 325 m, the bedrock appears shallower in the second profile than in the first one, suggesting that the bedrock topography is sloping to the southeast, while the weathering mantle thickens to that direction (Fig. 4). The highs of the bedrock surface in the second profile spatially correspond to zones of degradation of the ferricrete at 325–335 m and to a thinning of the saprolite separating a stream saturated zone from a domain of saturated saprolite between 5 and −15 m on the 'Middle-Glacis' (Fig. 4B).

The upper saprolite boundary is very corrugated in the first profile where it is overlain by a thin mottled zone, the layer boundaries being roughly parallel (Fig. 4A). The two weathering layers are shallower beneath the 'Middle-Glacis' than beneath the 'High-Glacis' over which the ferricrete and soft ferricrete layers are the thickest (Fig. 4). At 405 m and 705 m in the first section (Fig. 4A) and at 325 m in the second section (Fig. 4B), the bedrock surface highs or granitic domes corresponding to thinnings or discontinuities of saprolite are located just underneath the scarps that likely spring from degradation and partial removing of the overlying ferricrete at the edges of the 'High-Glacis'. On the other hand, the bedrock hollows correspond to weathering layer thickenings over which the ferruginous layers are also well developed, i.e., the ferricrete.

The groundsurface and bedrock topographies are controlled by weathering and erosion processes that determine the geomorphic patterns and the hydrodynamics of the underlying lateritic weathering mantle.

4.4. Geomorphic patterns vs. bedrock topography

The relationships between the groundsurface and the bedrock topographies are more clearly defined in Fig. 5 which is derived from Fig. 4. The vertical axis was expanded by a factor of ~3 to emphasize discrete groundsurface planforms of decametric size. At this length scale, convex bedrock domes correspond to groundsurface concavities while some topographic convexities overlie bedrock concavities as hollows. At the scale of hundreds of metres, the slope gradients for the two topographies are also negatively correlated (Fig. 5). At the whole profile scale, the bedrock and groundsurface topographies are effectively not parallel at all.

It was suggested that many tropical landscapes have undergone geomorphic modifications under the influence of climatic changes which control the balance between the weathering and erosion [1–6,23,29–34]. We also believe that climatic fluctuations were implied in the landscape evolution of southeastern Senegal; humid episodes favoured the rocks' weathering and the formation of ferricretes while the resulting landscape was eroded and dissected during dry periods, leading to new landforms, e.g., to the shaping of the 'High-Glacis' and 'Middle-Glacis' (Fig. 6). Fig. 6 represents the sequence of climate-depending processes that should have shaped the landforms of Tenkoto area. The previous lateritic weathering mantle developed in situ over the greenstone and the granitic bedrock was so eroded under semi-arid to

Fig. 4. Lithostratigraphic cross sections across the Tenkoto area based on ERT and cross-borehole data and physical parameters as discussed in the text: (A) profile I; (B) profile II. *SD* = saturated domain, $\rho < 130\ \Omega$ m; *S* = saprolite, $130 < \rho < 477\ \Omega$ m; *MZ* = mottled zone, $477 < \rho < 810\ \Omega$ m; *SF* = soft ferricrete, $810 < \rho < 2330\ \Omega$ m; *F* = ferricrete, $\rho > 2330\ \Omega$ m; *TZ* = transition zone, $417 < \rho < 713\ \Omega$ m; *WG* = less or more weathered granite, $710 < \rho < 3100\ \Omega$ m; *FG* = fresh granite, $\rho > 3140\ \Omega$ m. Vertical exaggeration in cross sections is 2.0.

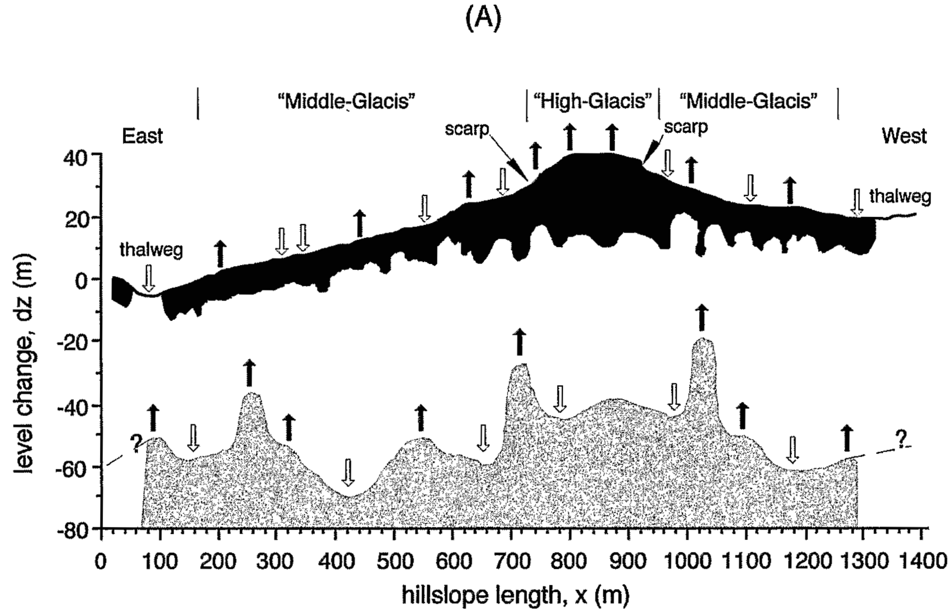

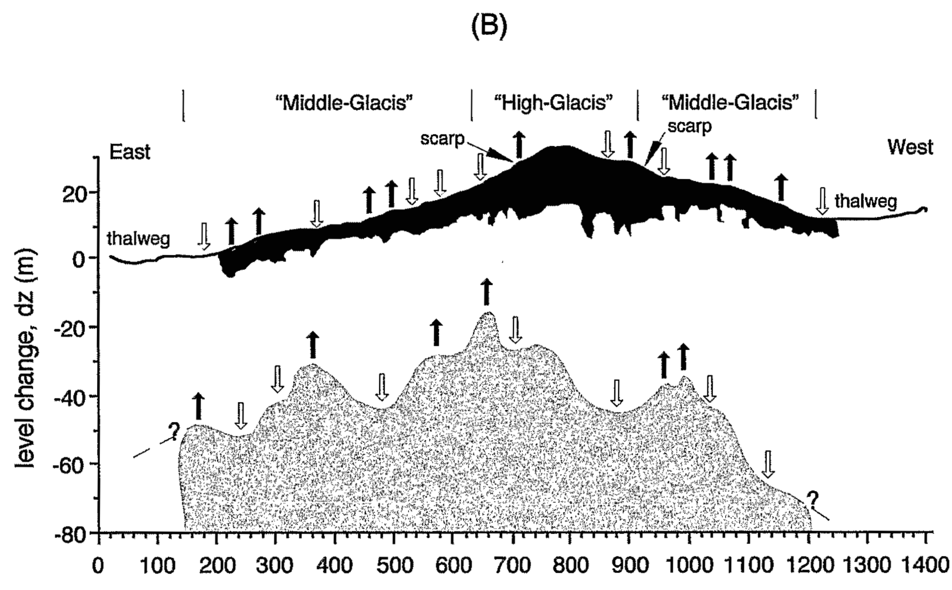

Fig. 5. Geomorphologic cross sections across the Tenkoto area derived from Fig. 4 after expansion of the vertical axis by a factor of ~3: (A) profile I; (B) profile II. Upper dark grey layer = soft ferricrete + ferricrete with $\rho > 810\ \Omega\,m$; lower light grey layer = weathered and unweathered granite with $\rho > 710\ \Omega\,m$; the space between the two layers is occupied by the saprolite + the mottled clay layer with $130 < \rho < 810\ \Omega\,m$, and by the saturated domain with $\rho < 130\ \Omega\,m$; black arrows = convex and plan-convex landforms + bedrock domes; white arrows = concave and plan-concave landforms + bedrock hollows.

arid climatic conditions, stripping and exposing some parts of the granitic bedrock, while the weathering profile capped with a thick ferricrete was partially preserved on greenstone (Fig. 6A). The resulting etched surface [31] probably exhibited concave and convex forms that controlled the accumulation patterns of the material eroded from the lateritic weathering profiles developed on the surrounding greenstones [23] (Fig. 6A,B); a relic of such profiles capped with a purple reddish massive ferricrete is still observable on the hill culminating at 283 m in the greenstone area (Fig. 1B). Coarse detritic materials embedding ferricrete debris with a similar petrographical facies have been observed over a thickness of $\sim$15 m in the 'High-Glacis' profiles [23] (Fig. 6C,D). Furthermore, the groundsurface of the peripheral hollows is strewn with blocks of that ferricrete and greenstone. Also, a part of the clay fraction of the fine detritic material should have been imported from the saprolite of the previous greenstone profiles.

Most of the coarse and fine materials first settled within the granitic bedrock concavities nearest to the western greenstones. Thick lateritic weathering profiles have been effectively developed above bedrock hollows in which the bulk of the eroded material coming from the surrounding greenstone hills should have been deposited (Fig. 6B–D). The resulting landforms carrying thick ferricretes are more convex than concave (Fig. 5). The ferricrete of the 'High-Glacis' is however less preserved, because it is more disaggregated in the second geo-electrical profile than in the first one. This can reflect the lesser thickness of the weathering profile since the bedrock slopes to the southeast while the groundsurface of the 'High-Glacis' slopes to the north, both with a gradient of $\sim$4% (Figs. 4 and 5). The bedrock surface is effectively shallower in the second profile than in the first one.

Under seasonal tropical conditions, the actual lateritic weathering mantle appears differentially eroded generating different topographic forms carrying distinct weathering facies: convex forms with thick ferricretes on the 'High-Glacis', plan-concave forms with soft ferricrete and/or mottled clays, and fairly concave forms with shallow mottled clays and saprolite, both being mainly developed on the 'Middle-Glacis', excepting the geomorphic scarps delimiting the 'High-Glacis' (Fig. 4). These scarps located just above bedrock domes present concavities with relatively small curvature radius, that may indicate the partial removal of the weathering mantle, and thus the thinning of the weathering profiles (Fig. 5). Thin profiles capped with a thin ferricrete or at best with a soft ferricrete are more sensitive to the erosion processes that create plan-concave landforms rather than convex. The 'Middle-Glacis' exhibits a succession of discrete concave and plan-convex forms that can reflect short distance transfers and deposits of colluvial materials which were effectively observed [23]. In such a way, the hillslope shape as a whole can be at once weathering and transport limited [30]. The convex 'High-Glacis' covered by thick ferricretes arises from creep processes, while the plan-concave slopes result from sheetwash and overland flow [30], which tend to truncate the weathering profiles. The above landforms and the physical properties of the associated materials are also able to control the permeability and thus the underlying hydrodynamics.

4.5. Hydrodynamics of the lateritic weathering mantle

The hydrodynamic processes are controlled by the groundsurface and bedrock topographies, and also by the physical properties of the materials, e.g., the porosity depending on clay and iron contents but also on size and content of residual quartz. Convex hillslope units with ferricrete generate divergent runoff while concave units favour the concentration of water as well as its infiltration since they result from the degradation of the ferricrete exhuming more porous mottled clays and saprolite. Beneath the resulting scarps, sharp bedrock domes act as structural thresholds generating divergent water fluxes and thus limiting the weathering processes, while adjacent concave bedrock forms as hollows concentrate the water fluxes enhancing the bedrock weathering (Fig. 5). These processes seasonally repeat so that the bedrock weathering process can be construed as a self-organized geochemical system. During the rainy season, a continuous saturated level in the saprolite of the second profile from −315 to 345 m just underneath the eastern scarp (Fig. 4B) would also be expected. Under seasonal tropical conditions, significant variations of the water table level can lead to underground dissolution processes [31], that could

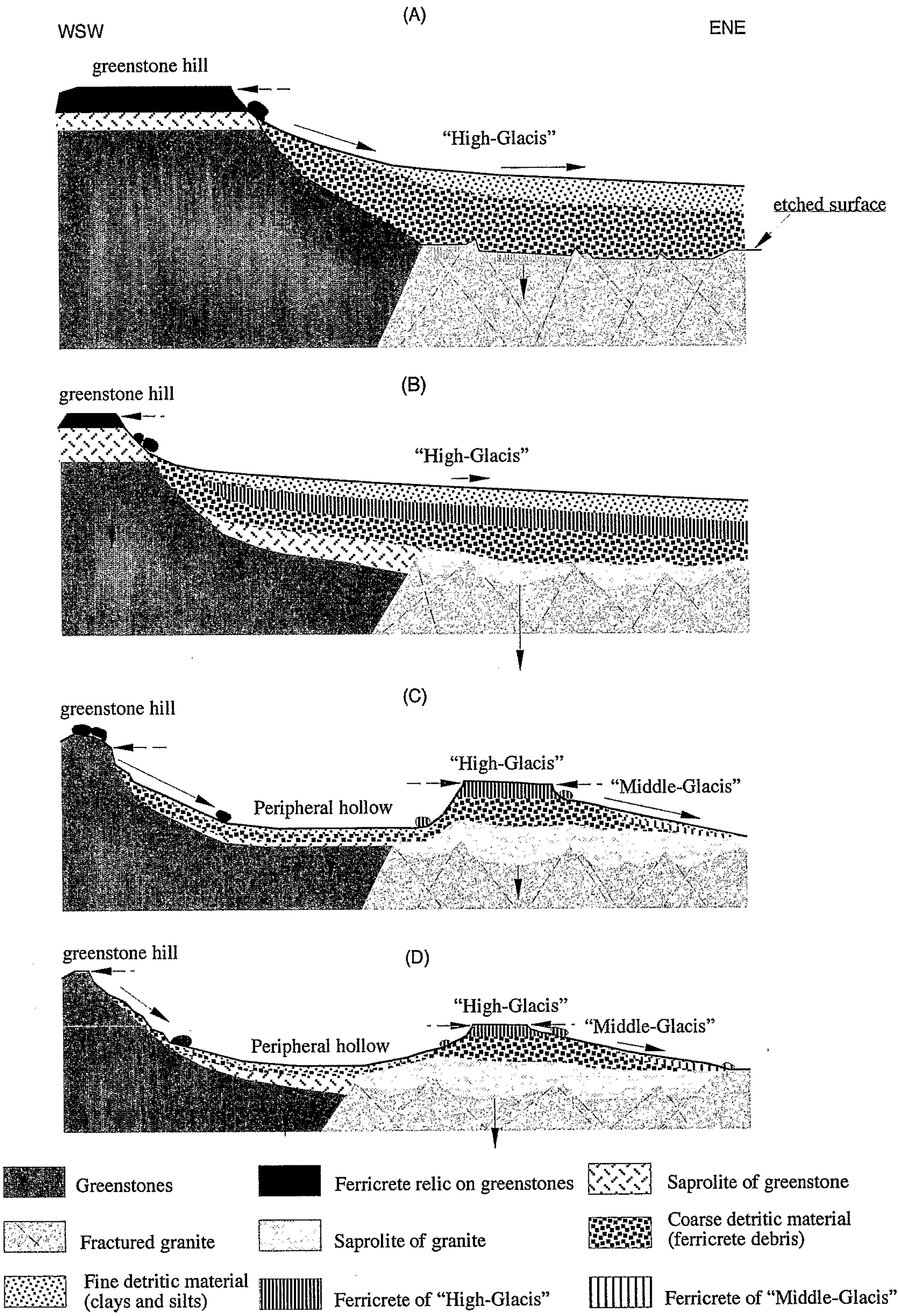
(A)
WSW
ENE
greenstone hill
"High-Glacis"
etched surface
(B)
greenstone hill
"High-Glacis"
(C)
greenstone hill
"High-Glacis"
"Middle-Glacis"
Peripheral hollow
(D)
greenstone hill
"High-Glacis"
"Middle-Glacis"
Peripheral hollow
Greenstones
Ferricrete relic on greenstones
Saprolite of greenstone
Fractured granite
Saprolite of granite
Coarse detritic material (ferricrete debris)
Fine detritic material (clays and silts)
Ferricrete of "High-Glacis"
Ferricrete of "Middle-Glacis"

also explain why the ferricrete of the 'High-Glacis' appears more disaggregated in the second profile than in the first one (Figs. 4 and 5).

5. Conclusion

2-D electrical resistivity tomography has proved useful in analyzing the layer organization of thick lateritic weathering mantles. Results from the ERT and cross-borehole methods along with the estimates of the aquifers and granitic rock resistivities provide constrained resistivity ranges for each weathering layer, i.e., the unweathered and weathered bedrock, the saturated and unsaturated saprolite, the mottled zone, the soft ferricrete and the ferricrete. That has also allowed useful description of the relationships between the layer boundaries, in particular between the granitic bedrock and the groundsurface topographies. The hillslope geomorphic patterns result from mechanical erosion processes of allochthonous material accumulated over an undulated granitic surface whose topography was shaped by previous climatic weathering processes. The spatial relationships between the bedrock and groundsurface topographies thus indicates that the hillslope shape results from both mechanical erosion and weathering processes reflecting climatic and geomorphic changes. Hence, the electrical resistivity tomography is a useful tool for earth investigations — it is also promising for mining and groundwater prospecting.

Acknowledgements

We gratefully thank J.-M. Wackerman for conductivity measurements in the pits and G. Grandin for helpful criticism on a previous version and advised hints for Figs. 1, 5 and 6. This work was financially supported by the 'Institut de Recherche pour le Développement', IRD (AB 662102, RED-UR06). Criticism and remarks from Pr. C.R. Twidale and an anonymous reviewer have been also appreciated. *[RV]*

Fig. 6. Sketch of weathering–erosion processes that should have governed the shaping of Tenkoto area landscape as a function of climatic changes: (A) semi-arid to arid climate; (B) humid seasonal tropical climate; (C) dry seasonal tropical to semi-arid climate; (D) actual seasonal tropical climate. Horizontal or oblique plain arrows = mechanical erosion with lateral transport of material; vertical plain arrows = rock weathering with thickening of the profile; dashed arrows = scarp retreat; the length of the arrows stands for the magnitude of processes; arbitrary scale for thicknesses; the topographic profile in (D) is that of Fig. 1B.

References

[1] G. Pedro, Distribution des principaux types d'altération chimique à la surface du globe, Présentation d'une esquisse géographique, Rev. Géogr. Phys. Dyn., Paris 10 (5) (1968) 457–470.

[2] B. Daily, C.R. Twidale, A.R. Milnes, The age of the lateritized summit surface on Kangaroo Island and adjacent areas of South Australia, J. Geol. Soc. Aust. 21 (4) (1974) 187–192.

[3] P. Michel, Cuirasses bauxitiques et ferrugineuses d'Afrique Occidentale, Aperçu chronologique, in: Géomorphologie des reliefs cuirassés dans les pays tropicaux chauds et humides, Travaux et Documents de Géographie tropicale, 33, CEGET, CNRS, Bordeaux, 1978, pp. 13–31.

[4] M.I. Bird, A.R. Chivas, Oxygen isotope dating of the Australian regolith, Nature 331 (1988) 513–516.

[5] Y. Tardy, Pétrologie des latérites et des sols tropicaux, Masson, Paris, 1993, 535 pp.

[6] C.R. Twidale, J.A. Bourne, Origin and age of bornhardts, southwest Western Australia, Aust. J. Earth Sci. 45 (1998) 903–914.

[7] D.B. Nahon, Introduction to the Petrology of Soils and Chemical Weathering, Wiley, New York, NY, 1991, 313 pp.

[8] A. Blot, J.C. Leprun, J.C. Pion, Originalité de l'altération et du cuirassement des dykes basiques dans le massif de granite de Saraya (Sénégal oriental), Bull. Soc. Geol. Fr. 7 (1976) 45–49.

[9] J.-C. Leprun, Les cuirasses ferrugineuses des pays cristallins de l'Afrique occidentale sèche, Genèse, Transformation, Dégradation, Mém. Sci. Géol., Strasbourg 58 (1979) 224 pp.

[10] D. Nahon, Cuirasses ferrugineuses et encroûtements calcaires au Sénégal occidental et en Mauritanie, Systèmes évolutifs: géochimie, structures, relais et coexistence, Mém. Sci. Géol., Strasbourg 44 (1976) 232 pp.

[11] D. Nahon, Evolution of iron crusts in tropical landscapes, in: S.M. Coleman, D.P. Dethier (Eds.), Rates of Chemical Weathering of Rock and Minerals, Academic Press, New York, NY, 1986, pp. 169–191.

[12] Y. Tardy, D. Nahon, Geochemistry of laterites, stability of Al-goethite, Al-hematite, and Fe^{3+}-kaolinite *in bauxites* and ferricretes: an approach to the mechanism of concretion formation, Am. J. Sci. 285 (1985) 865–903.

[13] J.-P. Ambrosi, D. Nahon, Petrological and geochemical

differentiation of lateritic iron crust profiles, Chem. Geol. 57 (1986) 371–393.
[14] A. Beauvais, F. Colin, Formation and transformation processes of iron duricrust systems under tropical humid environment, Chem. Geol. 106 (1993) 77–101.
[15] H. Robain, M. Descloitres, M. Ritz, Q.Y. Atangana, A multiscale electrical survey of a lateritic soil in the rain forest of Cameroon, J. Appl. Geophys. 34 (1996) 237–253.
[16] G.J. Palacky, K. Kadekaru, Effect of tropical weathering on electrical and electromagnetic measurements, Geophysics 44 (1979) 69–88.
[17] J.R.T. Hazell, C.R. Cratchley, C.R.C. Jones, The hydrogeology of crystalline aquifers in northern Nigeria and geophysical techniques used in their exploration, in: E.P. Wright, W.G. Burgers (Eds.), Hydrogeology of Crystalline Basement Aquifers in Africa, Geol. Soc. London, Spec. Publ. 66 (1992) 155–182.
[18] O. Koefoed, Geosounding Principles, 1, Resistivity Sounding Measurements, Elsevier, Amsterdam, 1979, 276 pp.
[19] G.V. Keller, F.C. Frischknecht, Electrical Methods in Geophysical Prospecting, Pergamon, Oxford, 1966, 519 pp.
[20] E. Delaitre, Etude des latérites du Sud-Mali par la méthode de sondage électrique, Ph.D. Thesis, Strasbourg University, Strasbourg, 1993, 193 pp.
[21] D.H. Griffiths, R.D. Barker, Two-dimensional resistivity imaging and modelling in areas of complex geology, J. Appl. Geophys. 29 (1993) 211–226.
[22] M. Ritz, J.-C. Parisot, S. Diouf, A. Beauvais, F. Diome, M. Niang, Electrical imaging of lateritic weathering mantles over granitic and metamorphic basement of eastern Senegal, West Africa, J. Appl. Geophys. 41 (1999) 335–344.
[23] P. Michel, Les bassins des fleuves Sénégal et Gambie, Etudes géomorphologiques, Mém. ORSTOM, Paris 63 (1973) 1170 pp.
[24] D.H. Griffiths, J. Turnbull, A.I. Olayinka, Two-dimensional resistivity mapping with a computer-controlled array, First Break 8 (1990) 121–129.
[25] L.P. Beard, G.W. Hohmann, A.C. Tripp, Fast resistivity/IP inversion using a low-contrast approximation, Geophysics 61 (1996) 169–179.
[26] M.H. Loke, R.D. Barker, Rapid least-squares inversion of apparent resistivity pseudosections by a quasi-Newton method, Geophys. Prosp. 44 (1996) 131–152.
[27] M.H. Loke, RES2DINV software user's manual, 1997.
[28] A. Hossin, Calcul des saturations en eau par la méthode des ciments argileux (formule d'Archie généralisée), Bull. A.F.T.P., 1960.
[29] G. Grandin, Aplanissements cuirassés et enrichissement des gisements de manganèse dans quelques régions d'Afrique de l'Ouest, Mém. Off. Rech. Sci. Tech. Outre-Mer, Fr. 82 (1976) 275 pp.
[30] M.J. Selby, Hillslope Materials and Processes, Oxford University Press, Oxford, 1993, 451 pp.
[31] M.F. Thomas, Geomorphology in the Tropics, A Study of Weathering and Denudation in Low Latitudes, Wiley, New York, NY, 1994, 460 pp.
[32] A. Beauvais, C. Roquin, Petrological differentiation patterns and geomorphic distribution of ferricretes in Central Africa, Geoderma 73 (1996) 63–82.
[33] Y. Tardy, C. Roquin, Dérive des continents, Paléoclimats et altérations tropicales, BRGM, Orléans, 1998, 473 pp.
[34] A. Beauvais, Geochemical balance of lateritization processes and climatic signatures in weathering profiles overlain by ferricretes in Central Africa, Geochim. Comochim. Acta (1999) in press.

REVISED NOTE TO CONTRIBUTORS 1 April 1997

1. Submission of manuscripts

Contributions should be sent to one of the editors. Four copies of the manuscript including photographs, line-drawings and tables should be submitted initially. Original line-drawings should *not* be sent until the final revised manuscript is submitted to the editor. Submission of an article is understood to imply that the article is original and unpublished and is not being considered for publication elsewhere. **Only the title page and abstract should be provided on diskette with the original submission; this will be used when e-mailing potential referees.** With the submitted manuscript, authors should enclose the names and addresses and fax, phone and e-mail numbers of five suggested reviewers. The editors will keep the identity of the reviewers anonymous but the reviewers may feel tree to correspond directly with the authors if they so desire. The responsibility for direct communication between the reviewer and the author must lie with the reviewer. **With a view to increasing the speed of publication authors are encouraged to revise within 6 weeks after receiving their reviews. At the editors' discretion, any revision received after this time limit may be regarded as a new submission that is subject to handling as a new paper.** Upon acceptance of an article by the journal, the author(s) will be asked to transfer the copyright of the article to the publisher. This transfer will ensure the widest possible dissemination of information. **There is an "Express Letter Section" for short, topical papers. The maximum permissible length is 5 journal pages and the total time from submission to publication will be ca. 3 months.** (a) *Submission of electronic text.* In order to publish the paper as quickly as possible, after acceptance authors are encouraged to submit the final text also on diskette. Please see the full instructions in the last issue of this volume. **Authors are encouraged to ensure that the diskette version and the hardcopy are identical — discrepancies can lead to publication of the wrong version.** (b) Authors are requested to provide details of a full corresponding address, telephone/fax and **e-mail numbers.**

2. Length of papers

THE MAXIMUM PERMISSIBLE LENGTH OF PAPERS IS 15 PRINTED JOURNAL PAGES. The average number of words on a (full) EPSL page = 580. Figures on a ratio of 1:1 (based on size). A WORD COUNT MUST BE PROVIDED ON THE TITLE PAGE OF MANUSCRIPTS. THERE ARE NO PAGE CHARGES.

3. Language

Manuscripts should be written in English only, and except for very short papers they should include a brief abstract.

4. Preparation of the text

(a) The manuscript should be prepared on a word processor and printed with double spacing and wide margins and include an abstract of not more than 500 words.
(b) Authors should use JUGS terminology. The use of S.I. units is also recommended.
(c) The title page should include the names of the authors, and their affiliation addresses and fax and e-mail numbers. In the case of more than one author please indicate to whom the correspondence should be addressed.

5. References

References should be limited to the minimum number necessary for citation of pertinent material. As a guide an average of 4 references per printed page can be used, **with a maximum of 50 references per article.** References to internal reports, etc., are to be avoided. (The statement "personal communication", with publication date in the text is preferable.)
References to the literature should strictly follow the journal's format: the references should be numbered in the order in which they are cited, and given in numerical sequence in the reference list at the end of the manuscript. The numbers should appear in the text in the appropriate places using numerals in square brackets on the line. In the reference list, periodicals [1], books [2], multi-author books [3] and proceedings [4], should be cited in accordance with the following examples:

1 I.M. Villa, J.C. Huneke, G.J. Wasserburg, ^{39}Ar recoil losses and presolar ages in Allende inclusions, Earth Planet. Sci. Lett. 63 (1983) 1–12.
2 I.S.E. Carmichael, F.J. Turner, J. Verhoogen, Igneous Petrology, McGraw-Hill, New York, NY, 1974, 739 pp.
3 S.R. Taylor, Chemical composition and evolution of the continental crust: the rare earth element evidence, in: M.W. McElhinney (Ed.), The Earth, its Origin, Structure and Evolution, Academic Press, London, 1978, pp. 2–44.
4 V.T. Bowen, H.D. Livingston, J.C. Burke, Distribution of transuranium nuclides in sediment and biota of the North Atlantic Ocean, in: Transuranium Elements in the Environment, IAEA Symp. Proc., 1976, pp. 107–120.

Abbreviations for titles of journals should follow the system used in the "Bibliographic Guide for Editors and Authors" published in 1974 by the American Chemical Society, Washington, DC.

6. Tables and illustrations

Tables should be compiled on separate sheets. A title should be provided for each table and they should be referred to in the text. Tables can also be sent as camera-ready versions to avoid errors in type-setting; a normal page-size reproduction of such tables should also be included in the manuscript. Efforts should be made to make the size of the tables correspond to the format of the journal (max. 15 × 20 cm).

(a) All illustrations should be numbered consecutively and referred to in the text.
(b) Each illustration should be lettered throughout, the size of the lettering being appropriate to that of the illustrations, but taking into account the possible need for reduction in size. The page format of the journal should be considered in designing the illustrations. All illustrations must be originals, in the form of glossy figures or laser prints. Each illustration must be accompanied by a photocopy
(c) Photographs must be of good quality, printed on glossy paper.
(d) Figure captions should be supplied on a separate sheet.
(e) Colour figures can be accepted providing the reproduction costs are met by the author. Please consult the publisher for further information.

7. Proofs

To achieve the high speed of publication, no proofs are sent to the authors. Manuscripts should therefore be prepared with the greatest possible care, and the submission of negatives for tabular materials in encouraged. Galley proofs may occasionally be obtained by making a special request to the editor, with the understanding that this implies delay in publication.

8. Fifty free reprints

Fifty reprints of each article published are supplied free of charge. A form for ordering extra reprints will be sent to the corresponding author on receipt of the accepted manuscript by the publisher.